

# Recognition of Seven Base Pair Sequences in the Minor Groove of DNA by Ten-Ring Pyrrole–Imidazole Polyamide Hairpins

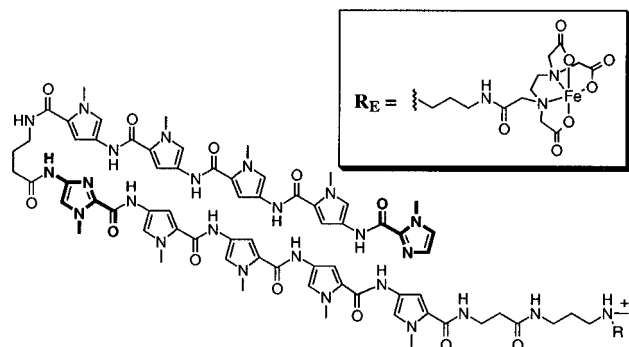
James M. Turner, Eldon E. Baird, and Peter B. Dervan\*

Contribution from the Division of Chemistry and Chemical Engineering,  
California Institute of Technology, Pasadena, California 91125

Received April 16, 1997<sup>⊗</sup>

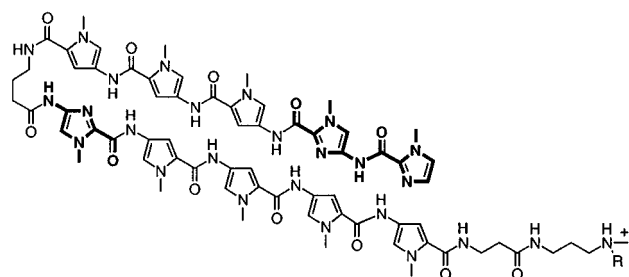
**Abstract:** A new upper limit of binding site size is defined for the hairpin polyamide–DNA motif. Ten-ring hairpin polyamides containing pyrrole (Py) and imidazole (Im) amino acids were designed for recognition of seven base pair (bp) sequences in the minor groove of DNA. The DNA binding properties of two polyamides, ImPyPyPyPy- $\gamma$ -ImPyPyPyPy- $\beta$ -Dp, and ImImPyPyPy- $\gamma$ -ImPyPyPyPy- $\beta$ -Dp were analyzed by footprinting and affinity cleavage on a DNA fragment containing the respective match sites 5'-TGTAACA-3' and 5'-TGGAAACA-3'. Quantitative footprint titrations demonstrate that ImPyPyPyPy- $\gamma$ -ImPyPyPyPy- $\beta$ -Dp binds the 7-bp match sequence 5'-TGTAACA-3' with an equilibrium association constant ( $K_a$ ) =  $1.2 \times 10^{10} \text{ M}^{-1}$  and 18-fold specificity versus the single base pair mismatch sequence 5'-TGGAAACA-3'. ImImPyPyPy- $\gamma$ -ImPyPyPyPy- $\beta$ -Dp differs from ImPyPyPyPy- $\gamma$ -ImPyPyPyPy- $\beta$ -Dp by a single amino acid substitution and binds its match 5'-TGGAAACA-3' site with  $K_a$  =  $3.6 \times 10^9 \text{ M}^{-1}$  and 300-fold specificity versus its corresponding single base pair mismatch sequence 5'-TGTAACA-3'. Ten-ring hairpin polyamides have binding affinities similar to those of eight-ring hairpin polyamides. These results indicate that the affinity of hairpin binding ceases to increase as the length of the polyamide subunits increases beyond four rings, analogous to the behavior of unlinked subunits. Therefore, recognition of seven base pairs by a ten-ring hairpin polyamide most likely represents an upper limit to the effective targetable site size of the hairpin polyamide–DNA motif.

Small molecules that target specific DNA sequences have the potential to control gene expression. Polyamides containing *N*-methylpyrrole and *N*-methylimidazole amino acids are synthetic ligands that have an affinity and specificity for DNA comparable to naturally occurring DNA binding proteins.<sup>1</sup> DNA recognition depends on side-by-side amino acid pairings in the minor groove. Antiparallel pairing of imidazole (Im) opposite pyrrole (Py) recognizes a G•C base pair, while a Py–Im combination recognizes C•G.<sup>2</sup> A Py–Py pair is degenerate and recognizes either an A•T or T•A base pair.<sup>2,3</sup> Four-ring polyamides covalently coupled to form eight-ring hairpin structures bind specifically to 6-bp target sequences and, importantly, have been shown to be cell permeable and to inhibit transcription of specific genes in cell culture.<sup>4</sup> The optimal binding site size for effective biological regulation has yet to be determined. This provides impetus to explore the binding site size limitations of the hairpin motif for recognition in the minor groove of DNA.<sup>5</sup> Given the failure of  $\geq$  five contiguous rings to maintain precise register with the DNA helix<sup>5</sup> combined with the constraint of covalent coupling, it remained to be determined if ten-ring hairpin polyamides could be successfully



1 R=CH<sub>3</sub>; ImPyPyPyPy- $\gamma$ -ImPyPyPyPy- $\beta$ -Dp

1-E•Fe(II) R=R<sub>E</sub>; ImPyPyPyPy- $\gamma$ -ImPyPyPyPy- $\beta$ -Dp-EDTA•Fe(II)



2 R=CH<sub>3</sub>; ImImPyPyPy- $\gamma$ -ImPyPyPyPy- $\beta$ -Dp

2-E•Fe(II) R=R<sub>E</sub>; ImImPyPyPy- $\gamma$ -ImPyPyPyPy- $\beta$ -Dp-EDTA•Fe(II)

**Figure 1.** Structures of the ten-ring polyamides and their EDTA derivatives synthesized by solid phase methods.

designed to recognize 7-bp sequences without compromising DNA-binding affinity or sequence specificity.

**Hairpin Polyamide.** In parallel with elucidation of the scope and limitations of the polyamide pairing rules, efforts have been

<sup>⊗</sup> Abstract published in *Advance ACS Abstracts*, August 1, 1997.

(1) Trauger, J. W.; Baird, E. E.; Dervan, P. B. *Nature* **1996**, *382*, 559.

(2) (a) Wade, W. S.; Mrksich, M.; Dervan, P. B. *J. Am. Chem. Soc.* **1992**, *114*, 8783. (b) Mrksich, M.; Wade, W. S.; Dwyer, T. J.; Geierstanger, B. H.; Wemmer, D. E.; Dervan, P. B. *Proc. Natl. Acad. Sci. U.S.A.* **1992**, *89*, 7586. (c) Wade, W. S.; Mrksich, M.; Dervan, P. B. *Biochemistry* **1993**, *32*, 11385.

(3) (a) Pelton, J. G.; Wemmer, D. E. *Proc. Natl. Acad. Sci. U.S.A.* **1989**, *86*, 5723. (b) Pelton, J. G.; Wemmer, D. E. *J. Am. Chem. Soc.* **1990**, *112*, 1393. (c) Chen, X.; Ramakrishnan, B.; Rao, S. T.; Sundaralingham, M. *Nature Struct. Biol.* **1994**, *1*, 169. (d) White, S.; Baird, E. E.; Dervan, P. B. *Biochemistry* **1996**, *35*, 12532.

(4) Gottesfield, J. M.; Nealy, L.; Trauger, J. W.; Baird, E. E.; Dervan, P. B. *Nature* **1997**, *387*, 202.

(5) Kelly, J. J.; Baird, E. E.; Dervan, P. B. *Proc. Natl. Acad. Sci. U.S.A.* **1996**, *93*, 6981.

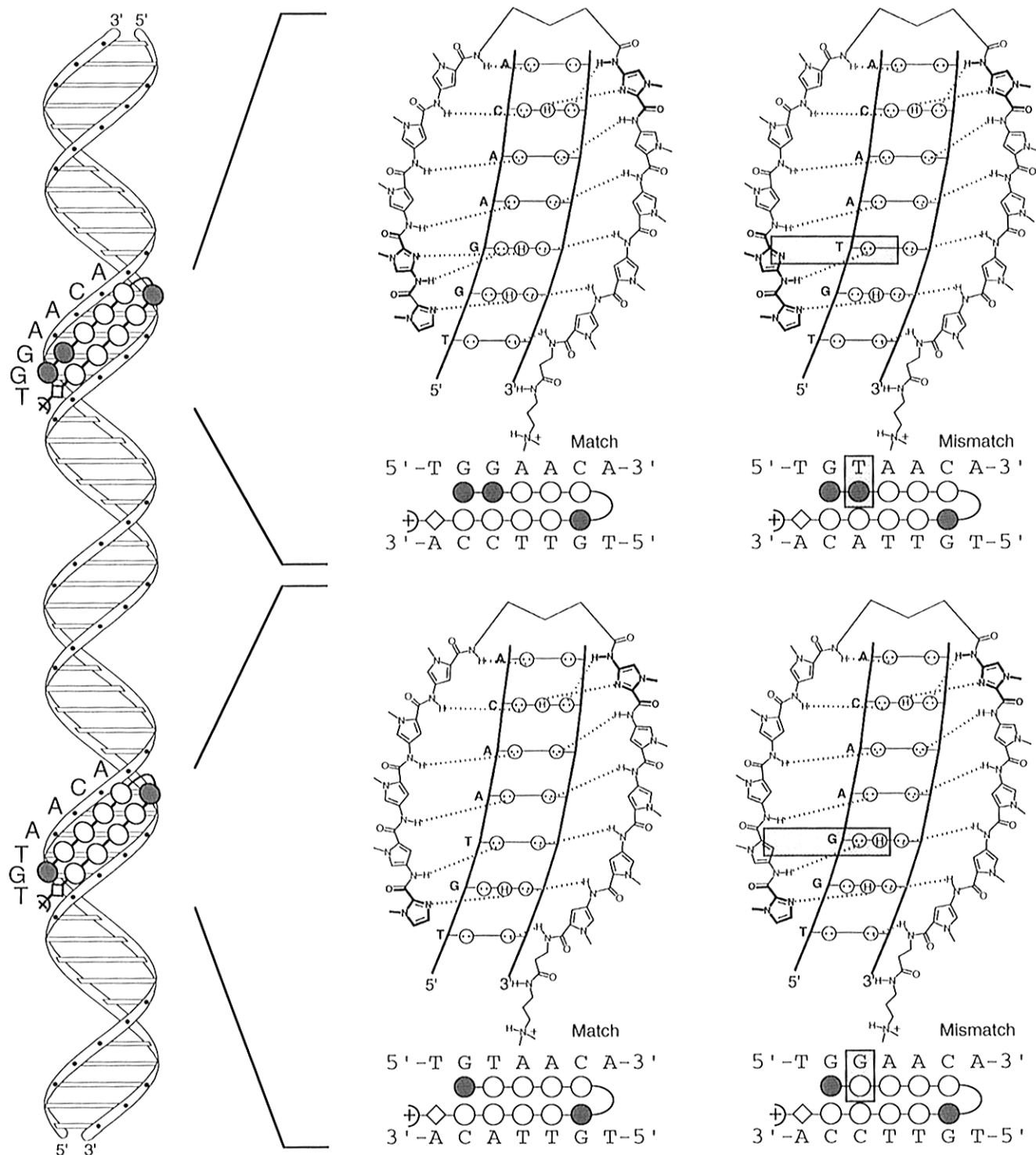


**Figure 2.** Binding model for the complexes formed between the DNA and either ImImPyPyPy- $\gamma$ -ImPyPyPyPy- $\beta$ -Dp (top) or ImPyPyPyPy- $\gamma$ -ImPyPyPyPy- $\beta$ -Dp (bottom). Circles with dots represent lone pairs of N3 of purines and O2 of pyrimidines. Circles containing an H represent the N2 hydrogen of guanine. Putative hydrogen bonds are illustrated by dotted lines. Ball and stick models are also shown. Shaded and nonshaded circles denote imidazole and pyrrole carboxamides, respectively. Nonshaded diamonds represent the  $\beta$ -alanine residue.

made to increase DNA-binding affinity and sequence specificity by covalently linking polyamide subunits.<sup>6–8</sup> A hairpin polyamide motif with  $\gamma$ -aminobutyric acid ( $\gamma$ ) serving as a turn-specific internal-guide-residue provides a synthetically accessible

method for C–N linkage of polyamide subunits.<sup>8</sup> Head-to-tail linked polyamides bind specifically to designated target sites

- (6) (a) Mrksich, M.; Dervan, P. B. *J. Am. Chem. Soc.* **1993**, *115*, 2572. (b) Geierstanger, B. H.; Dwyer, T. J.; Bathini, Y.; Lown, J. W.; Wemmer, D. E. *J. Am. Chem. Soc.* **1993**, *115*, 4474. (c) Geierstanger, B. H.; Jacobsen, J. P.; Mrksich, M.; Dervan, P. B.; Wemmer, D. E. *Biochemistry* **1994**, *33*, 3055. (7) (a) Mrksich, M.; Dervan, P. B. *J. Am. Chem. Soc.* **1994**, *116*, 3663. (b) Chen, Y. H.; Lown, J. W. *J. Am. Chem. Soc.* **1994**, *116*, 6995.

- (8) (a) Mrksich, M.; Parks, M. E.; Dervan, P. B. *J. Am. Chem. Soc.* **1994**, *116*, 7983. (b) Parks, M. E.; Baird, E. E.; Dervan, P. B. *J. Am. Chem. Soc.* **1996**, *118*, 6147. (c) Parks, M. E.; Baird, E. E.; Dervan, P. B. *J. Am. Chem. Soc.* **1996**, *118*, 6153. (d) Trauger, J. W.; Baird, E. E.; Dervan, P. B. *Chem. Biol.* **1996**, *3*, 369. (e) Swalley, S. E.; Baird, E. E.; Dervan, P. B. *J. Am. Chem. Soc.* **1996**, *118*, 8198. (f) Pilch, D. S.; Pokar, N. A.; Gelfand, C. A.; Law, S. M.; Breslauer, K. J.; Baird, E. E.; Dervan, P. B. *Proc. Natl. Acad. Sci. U.S.A.* **1996**, *93*, 8306. (g) de Claire, R. P. L.; Geierstanger, B. H.; Mrksich, M.; Dervan, P. B.; Wemmer, D. E. *J. Am. Chem. Soc.* In press.

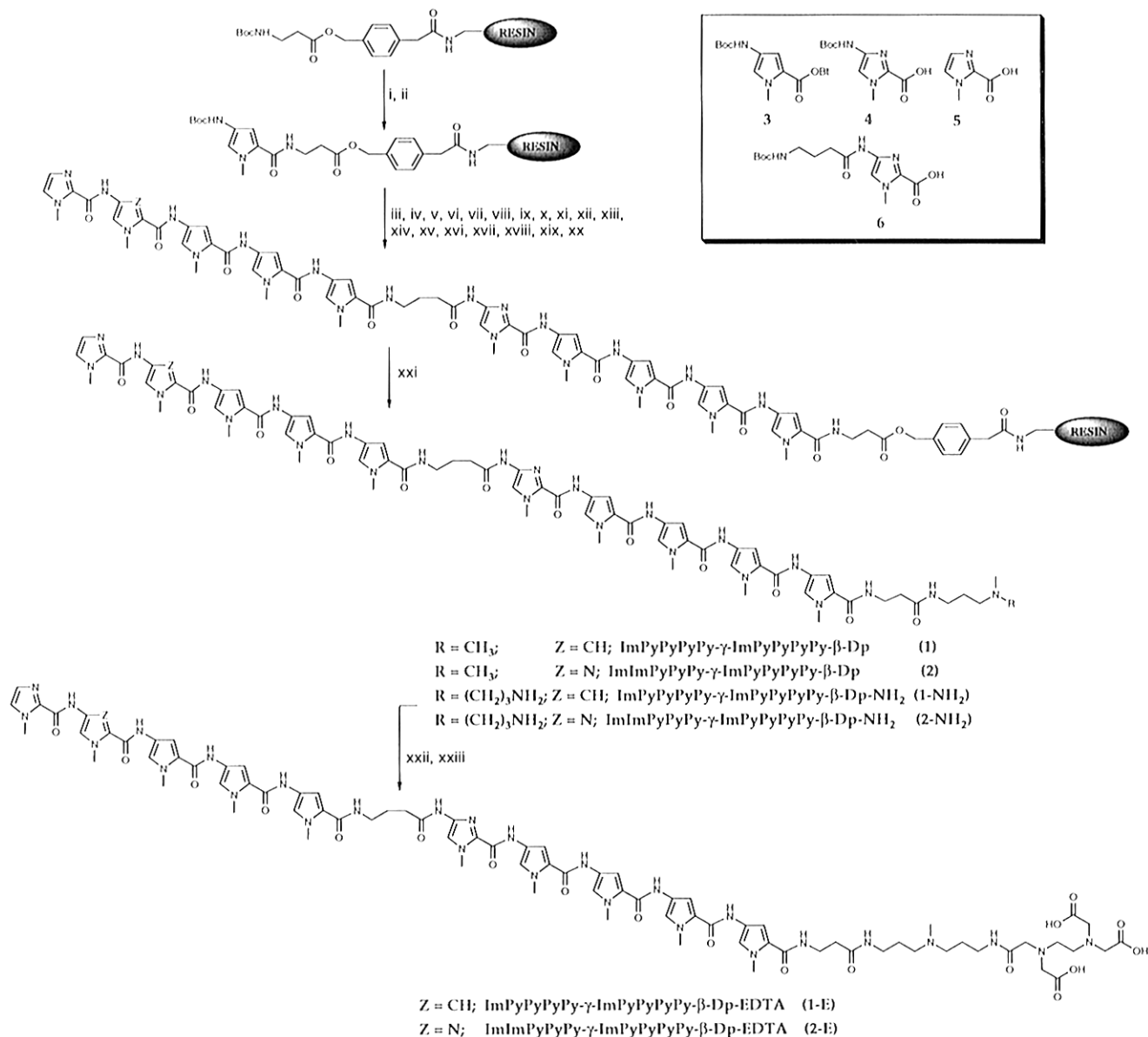


**Figure 3.** (Box) Pyrrole and imidazole monomers for synthesis of all compounds described here; Boc-Pyrrole-OBt ester **3**, Boc-Imidazole-acid **4**, imidazole-2-carboxylic acid **5**,<sup>2a</sup> and Boc- $\gamma$ -Imidazole-acid **6**. Solid phase synthetic scheme for ImPyPyPyPy- $\gamma$ -ImPyPyPyPy- $\beta$ -Dp, ImImPyPyPy- $\gamma$ -ImPyPyPyPy- $\beta$ -Dp, ImPyPyPyPy- $\gamma$ -ImPyPyPyPy- $\beta$ -Dp-NH<sub>2</sub>, ImImPyPyPy- $\gamma$ -ImPyPyPyPy- $\beta$ -Dp-NH<sub>2</sub>, ImPyPyPyPy- $\gamma$ -ImPyPyPyPy- $\beta$ -Dp-EDTA, and ImImPyPyPy- $\gamma$ -ImPyPyPyPy- $\beta$ -Dp-EDTA prepared from commercially available Boc- $\beta$ -alanine-Pam-resin (0.2 mmol/g): (i) 80% TFA/DCM, 0.4M PhSH; (ii) BocPy-OBt, DIEA, DMF; (iii) 80% TFA/DCM, 0.4M PhSH; (iv) BocPy-OBt, DIEA, DMF; (v) 80% TFA/DCM, 0.4M PhSH; (vi) BocPy-OBt, DIEA, DMF; (vii) 80% TFA/DCM, 0.4M PhSH; (viii) BocPy-OBt, DIEA, DMF; (ix) 80% TFA/DCM, 0.4M PhSH; (x) Boc- $\gamma$ -Im-OOH, (HBTU, DIEA), DMF; (xi) 80% TFA/DCM, 0.4M PhSH; (xii) BocPy-OBt, DIEA, DMF; (xiii) 80% TFA/DCM, 0.4M PhSH; (xiv) BocPy-OBt, DIEA, DMF; (xv) 80% TFA/DCM, 0.4M PhSH; (xvi) BocPy-OBt, DIEA, DMF; (xvii) 80% TFA/DCM, 0.4M PhSH; (xviii) BocPy-OBt, DIEA, DMF for **1**, Boc-Im-COOH (DCC, HOBT) for **2**; (xix) 80% TFA/DCM, 0.4M PhSH; (xx) imidazole-2-carboxylic acid (HBTU/DIEA); (xxi) *N,N*-dimethylaminopropylamine for **1** or **2**, or 3,3'-diamino-*N*-methylpropylamine for **1-NH<sub>2</sub>** or **2-NH<sub>2</sub>**, 55 °C; (xxii) EDTA-dianhydride, DMSO/NMP, DIEA, 55 °C; (xxiii) 0.1M NaOH.

with 100-fold enhanced affinities relative to unlinked subunits. A C-terminal  $\beta$ -alanine residue ( $\beta$ ) increases hairpin polyamide-DNA-binding affinity and specificity and facilitates solid phase synthesis.<sup>8b</sup> The hairpin model is supported by footprinting, affinity cleaving, and NMR structure studies.<sup>1,3d,8</sup>

To expand the targetable binding site size and sequence repertoire of the hairpin polyamide motif, two polyamides containing either two or three Im amino acid residues, ImPyPyPyPy- $\gamma$ -ImPyPyPyPy- $\beta$ -Dp (**1**) and ImImPyPyPy- $\gamma$ -ImPyPyPyPy- $\beta$ -Dp (**2**) (Dp = dimethylaminopropylamide), were synthesized by solid phase methods (Figure 1).<sup>9</sup> The corresponding EDTA analogs ImPyPyPyPy- $\gamma$ -ImPyPyPyPy- $\beta$ -Dp-

EDTA (**1-E**) and ImImPyPyPy- $\gamma$ -ImPyPyPyPy- $\beta$ -Dp-EDTA (**2-E**) were also constructed to confirm the orientation of the hairpin motif at each binding site. We report here the DNA-binding affinity, orientation, and sequence selectivity of two ten-ring hairpin polyamides, ImPyPyPyPy- $\gamma$ -ImPyPyPyPy- $\beta$ -Dp (**1**) and ImImPyPyPy- $\gamma$ -ImPyPyPyPy- $\beta$ -Dp (**2**), for two respective 7-bp target sequences, 5'-TGTAACA-3' and 5'-TGGAACA-3' (Figure 2). Three separate techniques are used to characterize the DNA-binding properties of the designed polyamides: methidiumpropyl-EDTA-Fe(II) (MPE-Fe(II)) footprinting,<sup>10</sup> affinity cleaving,<sup>11</sup> and DNase I footprinting.<sup>12</sup> Information about

(9) Baird, E. E.; Dervan, P. B. *J. Am. Chem. Soc.* **1996**, *118*, 6141.

(10) (a) Van Dyke, M. W.; Dervan, P. B. *Nucl. Acids Res.* **1983**, *11*, 5555. (b) Van Dyke, M. W.; Dervan, P. B. *Science* **1984**, *225*, 1122.

5' -AATTCGAGCTCGGTACCCGGGATCGCGAGCTCAT**TGTAACAGCGAGCTCAT**TGGAACAGCGAGCTCATAGCTTGGCGTAATCATGGTCATAGCT****  
 3' -TTAAGCTCGAGCCATGGGCCCTAGCGCTCGAGTA**ACAT**TGTCGCTCGAGTA**ACCTTGT******CGCTCGAGTATCGAACCCGATTAGTACCAGTATCGA

GTTCCTGTGTGAAATGTTATCCGCTCACAATTCACACAACATACGAGCCGGAAGCATAAAGTGTAAGCCTGGGGTGCCTAATGAGTGAGCTAAC  
 CAAAGGACACACTTTAACAAATAGCGAGTGTTAAGGTGTGTGTATGCTCGGCCTTCGTATTTACATTTCCGACCCCAAGGATTACTACTCGATTG

TCACATTCCTTFCGCTGCGCTCACTGCCCCGCTTTCAGTCGGGAAACCTGTCGTGCCAG-3'  
 AGTGTAAATTAACGCAACGCGAGTGACGGGCGAAAGGTCAGCCCTTTGGACAGCACGGTC-5'

**Figure 4.** Sequence of the 252 bp pJK7 *EcoRI/PvuII* restriction fragment. The two binding sites that were analyzed in quantitative footprint titration experiments are indicated.

precise binding site size is gained from MPE·Fe(II) footprinting, while affinity cleavage studies determine the binding orientation and stoichiometry of the 1:1 hairpin:DNA complex. Quantitative DNase I footprint titrations allow determination of equilibrium association constants ( $K_a$ ) of the polyamides for respective match and mismatch binding sites.

## Results and Discussion

**Synthesis of Polyamides.** The polyamides ImPyPyPyPy- $\gamma$ -ImPyPyPyPy- $\beta$ -Dp (**1**) and ImImPyPyPy- $\gamma$ -ImPyPyPyPy- $\beta$ -Dp (**2**) were synthesized in a stepwise manner from Boc- $\beta$ -alanine-Pam resin (1 g resin, 0.2 mmol/g substitution) using Boc-chemistry machine-assisted protocols in 21 steps (Figure 3). The  $\gamma$ -Im subunit was introduced to both polyamides as a dimer-block in order to avoid the slow coupling of  $\gamma$  to Im. A sample of resin (240 mg) was then cleaved by a single-step aminolysis reaction with ((dimethylamino)propyl)amine (55 °C, 18 h) and subsequently purified by reversed phase HPLC to provide ImPyPyPyPy- $\gamma$ -ImPyPyPyPy- $\beta$ -Dp (**1**, 13 mg) and ImImPyPyPy- $\gamma$ -ImPyPyPyPy- $\beta$ -Dp (**2**, 11 mg). For the synthesis of analogs modified with EDTA, a sample of resin was cleaved with 3,3'-diamino-*N*-methylpropylamine (55 °C) and purified by reversed phase HPLC to provide either ImPyPyPyPy- $\gamma$ -ImPyPyPyPy- $\beta$ -Dp-NH<sub>2</sub> (**1-NH<sub>2</sub>**, 31 mg) or ImImPyPyPy- $\gamma$ -ImPyPyPyPy- $\beta$ -Dp (**2-NH<sub>2</sub>**, 29 mg). **1-NH<sub>2</sub>** and **2-NH<sub>2</sub>** afford a primary amine group suitable for modification. The polyamide amine was treated with an excess of EDTA-dianhydride (DMSO/NMP, DIEA, 55 °C, 15 min), and the remaining anhydride hydrolyzed (0.1 M NaOH, 55 °C, 10 min). The EDTA modified polyamides ImPyPyPyPy- $\gamma$ -ImPyPyPyPy- $\beta$ -Dp-EDTA (**1-E**, 5 mg) and ImImPyPyPy- $\gamma$ -ImPyPyPyPy- $\beta$ -Dp-EDTA (**2-E**, 6 mg) were then isolated by HPLC chromatography. The synthesis of **1**, **1-NH<sub>2</sub>**, **1-E**, **2**, **2-NH<sub>2</sub>**, and **2-E** is outlined in Figure 3. Ten-ring hairpin polyamides are soluble at concentrations  $\leq 1$  mM and can be rapidly prepared by solid phase methods in sufficient quantity and purity for biological applications.

**Identification of Binding Site Size by MPE·Fe(II) Footprinting.** MPE·Fe(II) footprinting on the 3'- and 5'-<sup>32</sup>P end-labeled 252 base pair *EcoRI/PvuII* restriction fragment from the plasmid pJK7<sup>5</sup> (25 mM Tris-acetate, 10 mM NaCl, 100  $\mu$ M calf thymus DNA, pH 7.0, 22 °C) reveals that the polyamides, each at 1  $\mu$ M concentration, are binding to their designated match sites (Figures 4 and 5).<sup>10</sup> Mismatch sites are observed at higher polyamide concentration.<sup>13</sup> Footprinting patterns reveal asymmetrically 3'-shifted protection of 7-bp sites (Figure 6). MPE·Fe(II) protection patterns are consistent with formation

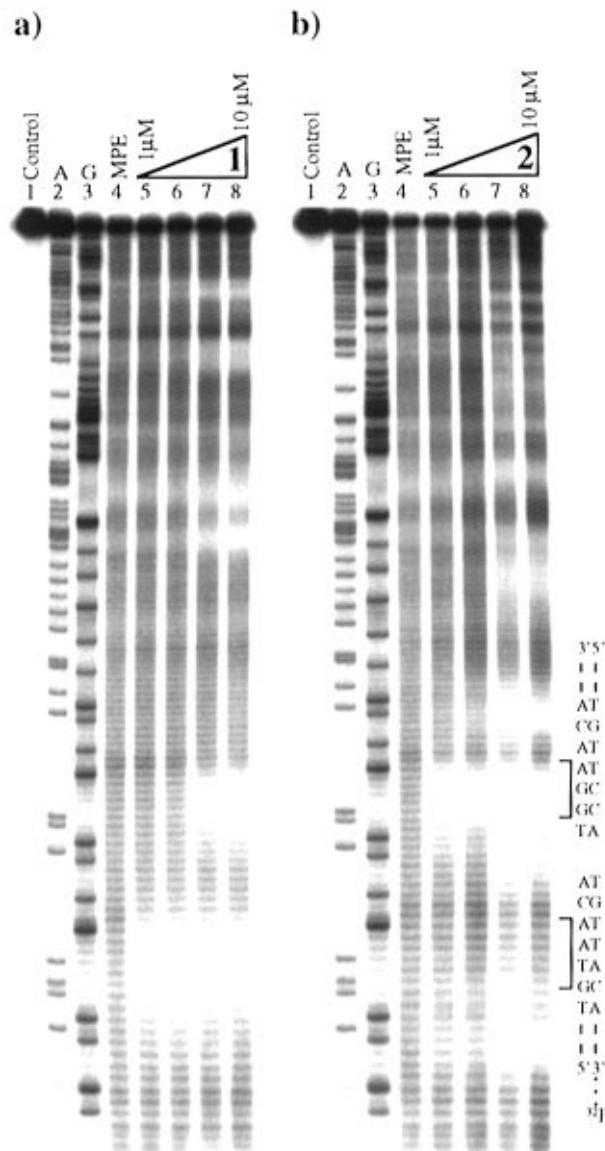


**Figure 5.** MPE·Fe(II) footprinting on a 3'-<sup>32</sup>P-labeled 252 bp *EcoRI/PvuII* restriction fragment from plasmid pJK7. The 5'-TGTAACA-3' and 5'-TGGAACA-3' sites are shown on the right side of the autoradiogram. Lane 1, intact DNA; lane 2, A reaction; lane 3, G reaction; lane 4, MPE·Fe(II) standard; lane 5, 1  $\mu$ M **1** or **2**; lane 6, 2  $\mu$ M **1** or **2**; lane 7, 5  $\mu$ M **1** or **2**; lane 8, 10  $\mu$ M **1** or **2**. All lanes contain 15 kcpm 3'-radiolabeled DNA and 25 mM Tris-acetate buffer (pH 7.0), 10 mM NaCl, and 100  $\mu$ M/base pair calf thymus DNA.

of a 1:1 hairpin polyamide–DNA complex in the minor groove. Polyamide **1** at 5  $\mu$ M concentration protects both the cognate 5'-TGTAACA-3' site and the single-base-pair mismatch 5'-TGGAACA-3' site. At 5  $\mu$ M concentration, polyamide **2** protects its cognate 5'-TGGAACA-3' site; however, no protection is observed at the 5'-TGTAACA-3' single base pair mismatch site. Instead polyamide **2** is found to preferentially protect a 5'-AGCTCAT-3' double base pair mismatch site

(11) (a) Taylor, J. S.; Schultz, P. G.; Dervan, P. B. *Tetrahedron* **1984**, 40, 457. (b) Dervan, P. B. *Science* **1986**, 232, 464.

(12) (a) Brenowitz, M.; Senear, D. F.; Shea, M. A.; Ackers, G. K. *Methods Enzymol.* **1986**, 130, 132. (b) Brenowitz, M.; Senear, D. F.; Shea, M. A.; Ackers, G. K. *Proc. Natl. Acad. Sci. U.S.A.* **1986**, 83, 8462. (c) Senear, D. F.; Brenowitz, M.; Shea, M. A.; Ackers, G. K. *Biochemistry* **1986**, 25, 7344.

(13) We note that no conclusion regarding polyamide binding affinities can be drawn from these experiments due to specific and nonspecific interactions of the polyamides with the calf thymus carrier DNA.

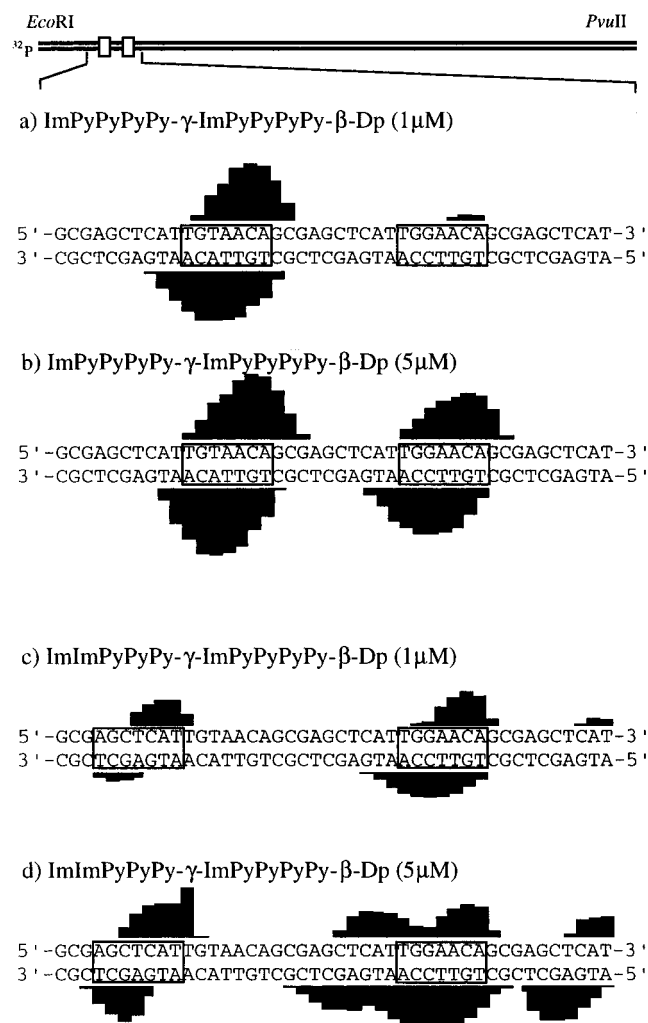


**Figure 6.** Results from MPE·Fe(II) footprinting of ImPyPyPyPy- $\gamma$ -ImPyPyPyPy- $\beta$ -Dp and ImImPyPyPy- $\gamma$ -ImPyPyPyPy- $\beta$ -Dp. (Top) Illustration of the 252 bp restriction fragment with the position of the sequence indicated. Boxes represent equilibrium binding sites determined by the published model. Only sites that were quantitated by DNase I footprint titrations are boxed. (a) and (c): MPE·Fe(II) protection patterns for polyamides at 1  $\mu$ M concentration. (b) and (d): MPE·Fe(II) protection patterns for polyamides at 5  $\mu$ M concentration. Bar heights are proportional to the relative protection from cleavage at each band.

present in the repeated 10-bp sequence which flanks each of the designated binding sites.

**Determination of Binding Orientation and Stoichiometry by Affinity Cleaving.** Affinity cleavage experiments were performed on a 3'- and 5'- $^{32}$ P end-labeled *EcoRI/PvuII* restriction fragment from the plasmid pJK7<sup>5</sup> (20 mM HEPES, 200 mM NaCl, 50  $\mu$ g/mL glycogen, pH 7.0, 22  $^{\circ}$ C) (Figures 7 and 8).<sup>11</sup> Affinity cleavage experiments were performed with analogs of polyamides **1** and **2** modified with an EDTA·Fe(II) moiety at the carboxy terminus. The observed cleavage patterns are in all cases 3' shifted, consistent with location of the polyamide in the minor groove.<sup>11</sup>

Affinity cleavage patterns reveal that at 1 and 10 nM concentrations, the homodimeric polyamide **1-E** binds its symmetrical target site 5'-TGTAACA-3' in two distinct orientations, as expected (Figure 9). Despite the symmetry of the 7-bp target site around the central A·T base pair, an apparent 2-fold orientational preference is observed, indicating that the sequences flanking the 7-bp site affect complex stability. The orientation preference is likely due to sequence-dependent

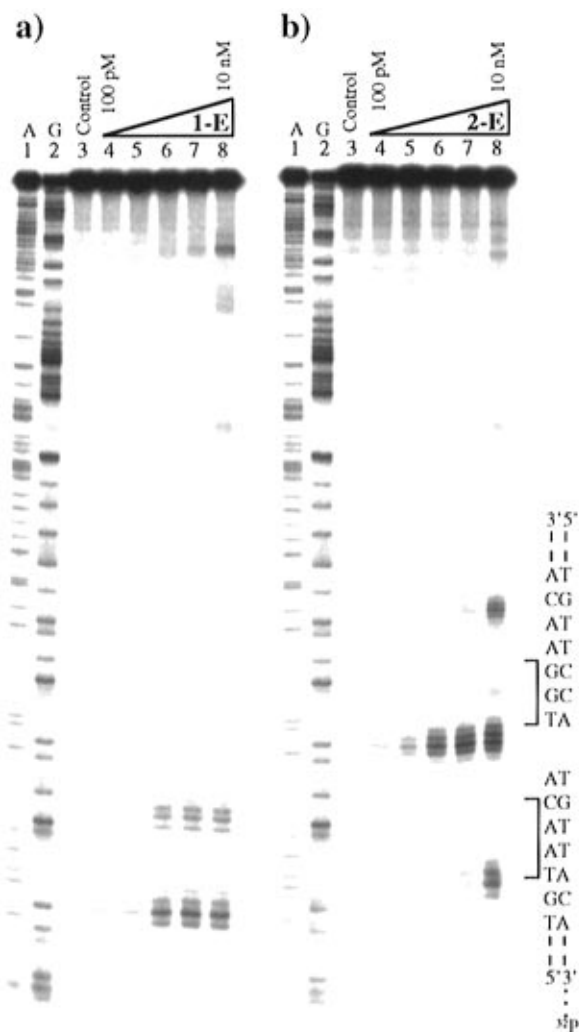


**Figure 7.** Affinity cleavage experiments on a 3'- $^{32}$ P-labeled 252 bp *EcoRI/PvuII* restriction fragment from plasmid pJK7. The 5'-TGTAACA-3' and 5'-TGGAACA-3' sites are shown on the right side of the autoradiogram. Lane 1, A reaction; lane 2, G reaction; lane 3, intact DNA; lane 4, 100 pM **1-E** or **2-E**; lane 5, 300 pM **1-E** or **2-E**; lane 6, 1 nM **1-E** or **2-E**; lane 7, 3 nM **1-E** or **2-E**; lane 8, 10 nM **1-E** or **2-E**. All lanes contain 15 kcpm 3'-radiolabeled DNA. The affinity cleavage lanes (3–8) contain 20 mM HEPES (pH 7.0), 200 mM NaCl and 50  $\mu$ g/mL glycogen.

interactions of the polyamide tail which extends beyond the 7-bp binding site. Binding of **1-E** with the tail at the 5'-side of the 5'-catTGTAACAgcg-3' binding site places the C-terminus approximately opposite a T·A base pair, whereas binding with the tail of the polyamide opposite the 3'-side of the binding site places the C-terminal  $\beta$ -alanine residue opposite a G·C base pair. The observed orientation preference may result from a steric interaction between the C-terminal  $\beta$ -alanine residue and the exocyclic 2-amino group of guanine. It is unlikely that the observed orientation preference results from a specific interaction with the central A·T base pair of the binding site.<sup>3d</sup>

In the presence of 1 nM **2-E** a single cleavage locus is observed proximal to the 5'-side of the binding site for the heterodimeric polyamide **2-E** binding its designated target site 5'-TGGAACA-3, indicating that the terminus of the polyamide is located at the 5'-side of the binding site. The observation of a single cleavage locus is consistent only with an oriented 1:1 complex and rules out any 2:1 overlapped or extended binding motifs.<sup>14</sup> In the presence of 10 nM polyamide **2-E** additional cleavage loci are revealed which result from polyamide binding in the 10-bp intervening sequence between binding sites. The

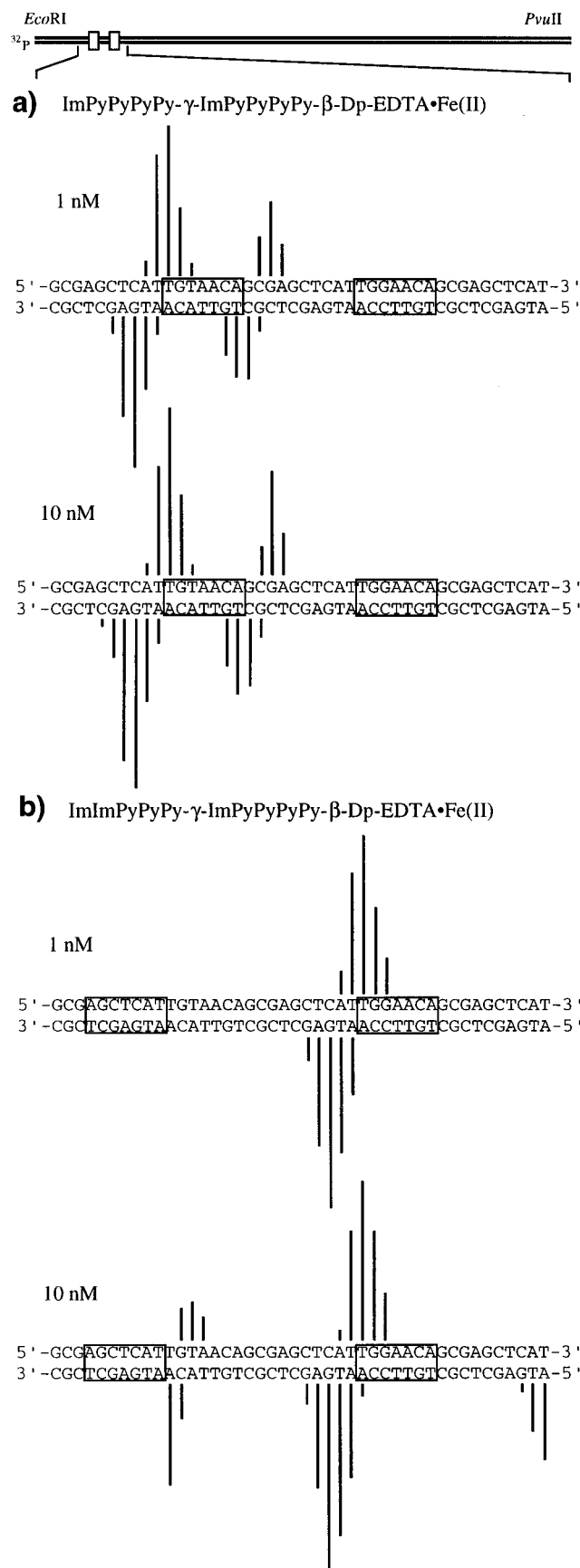


**Figure 8.** Affinity cleavage patterns of (a) ImPyPyPyPy- $\gamma$ -ImPyPyPyPy- $\beta$ -Dp-EDTA·Fe(II) and (b) ImImPyPyPy- $\gamma$ -ImPyPyPyPy- $\beta$ -Dp-EDTA·Fe(II) at 1 and at 10 nM. Bar heights are proportional to the relative cleavage intensities at each base pair.

observed cleavage patterns combined with the MPE·Fe(II) footprinting results described above allow putative assignment

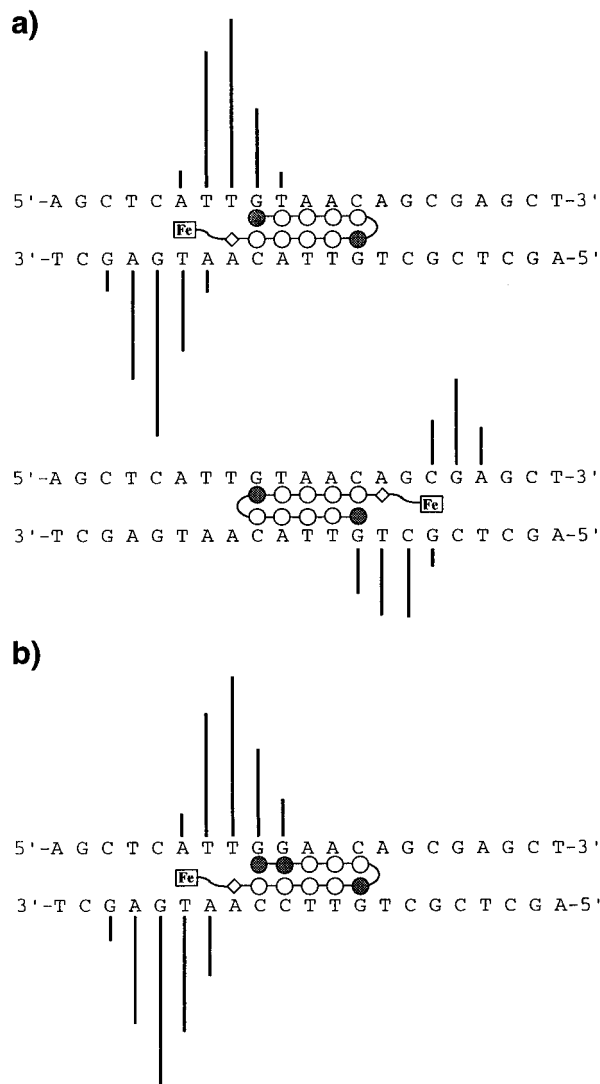


**Figure 9.** Affinity cleavage patterns and ball and stick models of the ten-ring EDTA·Fe(II) analogs **1-E** (a) and **2-E** (b) bound to their formal match sites. Bar heights are proportional to the relative cleavage intensities at each base pair. Shaded and nonshaded circles denote imidazole and pyrrole carboxamides, respectively. Nonshaded diamonds represent the  $\beta$ -alanine residue. The boxed Fe denotes the EDTA·Fe(II) cleavage moiety. (a) Symmetric binding to a formal match sequence by ImPyPyPyPy- $\gamma$ -ImPyPyPyPy- $\beta$ -Dp-EDTA·Fe(II) at 1 nM. (b) Single orientation binding to a formal match sequence by ImImPyPyPy- $\gamma$ -ImPyPyPyPy- $\beta$ -Dp-EDTA·Fe(II) at 1 nM.

of the mismatch polyamide binding site as the double base pair mismatch site 5'-AGCTCAT-3'.

**Determination of Binding Affinities by Quantitative DNase I Footprinting.** Quantitative DNase I footprint titration experiments (10 mM Tris-HCl, 10 mM KCl, 10 mM MgCl<sub>2</sub> and 5 mM CaCl<sub>2</sub>, pH 7.0, 22 °C) were performed to determine the equilibrium association constants of the polyamides for the two bound sites (Table 1).<sup>12</sup> ImPyPyPyPy- $\gamma$ -ImPyPyPyPy- $\beta$ -Dp binds its match site 5'-TGTAACA-3' with an equilibrium association constant of  $K_a = 1.2 \times 10^{10} \text{ M}^{-1}$  (Figures 10 and 11). The sequence 5'-TGGAAACA-3' is bound with 18-fold lower affinity ( $K_a = 6.8 \times 10^8 \text{ M}^{-1}$ ) (Table 1). ImImPyPyPy- $\gamma$ -ImPyPyPyPy- $\beta$ -Dp binds its 5'-TGGAAACA-3' match site with an equilibrium association constant of  $K_a = 3.6 \times 10^9 \text{ M}^{-1}$ . The internal mismatch 5'-TGTAACA-3' site is bound with at

(14) (a) Trauger, J. W.; Baird, E. E.; Mrksich, M.; Dervan, P. B. *J. Am. Chem. Soc.* **1996**, *118*, 6160. (b) Geierstanger, B. H.; Mrksich, M.; Dervan, P. B.; Wemmer, D. E. *Nature Struct. Biol.* **1996**, *3*, 321.

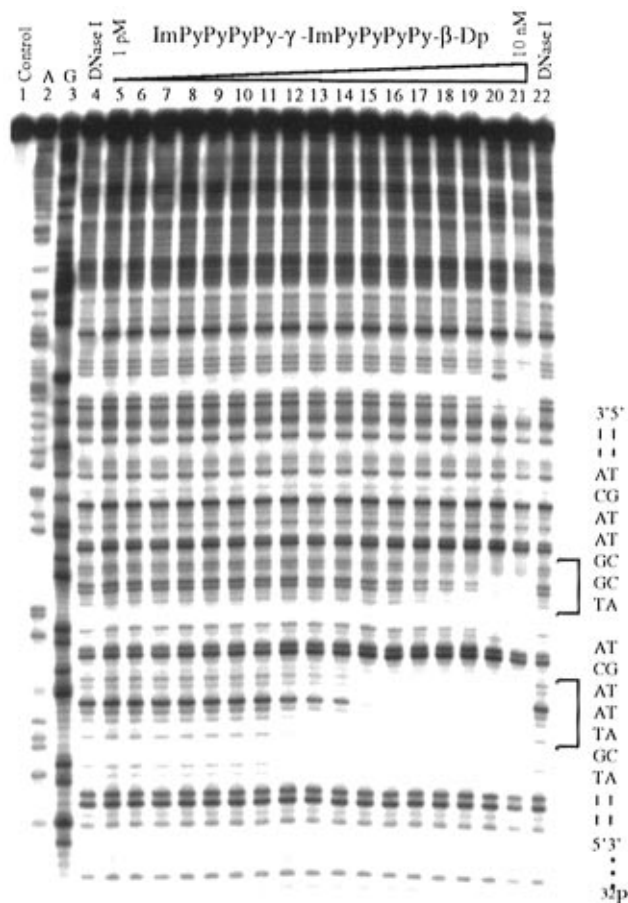


**Figure 10.** Quantitative DNase I footprint titration experiment with ImPyPyPyPy- $\gamma$ -ImPyPyPyPy- $\beta$ -Dp on the *EcoRI/PvuII* restriction fragment from plasmid pJK7: lane 1, intact DNA; lane 2, A reaction; lane 3, G reaction; lane 4, DNase I standard; lanes 5–21, 1 pM, 2 pM, 5 pM, 10 pM, 15 pM, 25 pM, 40 pM, 65 pM, 100 pM, 150 pM, 250 pM, 400 pM, 650 pM, 1 nM, 2 nM, 5 nM, 10 nM ImPyPyPyPy- $\gamma$ -ImPyPyPyPy- $\beta$ -Dp; lane 22, DNase I standard. The 5'-TGTAACA-3' and 5'-TGGAACA-3' sites that were analyzed are shown on the right side of the autoradiogram. All reactions contain 15 kcpm restriction fragment, 10 mM Tris-HCl (pH 7.0), 10 mM KCl, 10 mM MgCl<sub>2</sub>, and 5 mM CaCl<sub>2</sub>.

least 300-fold lower affinity ( $K_a < 1 \times 10^7 \text{ M}^{-1}$ ). In addition to the designated match and mismatch sites, polyamide **2** is observed to bind the unexpected 5'-AGCTCAT-3' mismatch site identified by affinity cleavage and MPE·Fe(II) footprinting experiments described above with  $K_a = 7.5 \times 10^8 \text{ M}^{-1}$ . The reduced overall specificity and binding affinity of polyamide **2** relative to polyamide **1** most likely results from the presence of a 5'-GA-3' step in the match target site. A 5'-GA-3' step has recently been observed to reduce polyamide binding affinities by approximately 10-fold.<sup>3d</sup>

Based on the pairing rules for polyamide-DNA complexes, the sites 5'-TGTAACA-3' and 5'-TGGAACA-3' are for polyamide **1** "match" and "single-base-pair-mismatch sites", respectively and for polyamide **2** "single-base-pair-mismatch" and "match sites" respectively (Figure 2). The specificity of polyamides **1** and **2** for their respective match sites results from very small structural changes (Figure 1). Replacing a single C-H in **1** with a nitrogen atom as in **2** reduces the affinity of the ImImPyPyPy- $\gamma$ -ImPyPyPyPy- $\beta$ -Dp·5'-TGTAACA-3' complex relative to the ImPyPyPyPy- $\gamma$ -ImPyPyPyPy- $\beta$ -Dp·5'-TGTAACA-3' complex by >1200-fold, a free energy difference of at least 4 kcal/mol. Similarly, replacing a N in **2** with a C-H as in **1** reduces the affinity of the ImPyPyPyPy- $\gamma$ -ImPyPyPyPy- $\beta$ -Dp·5'-TGGAACA-3' complex relative to the

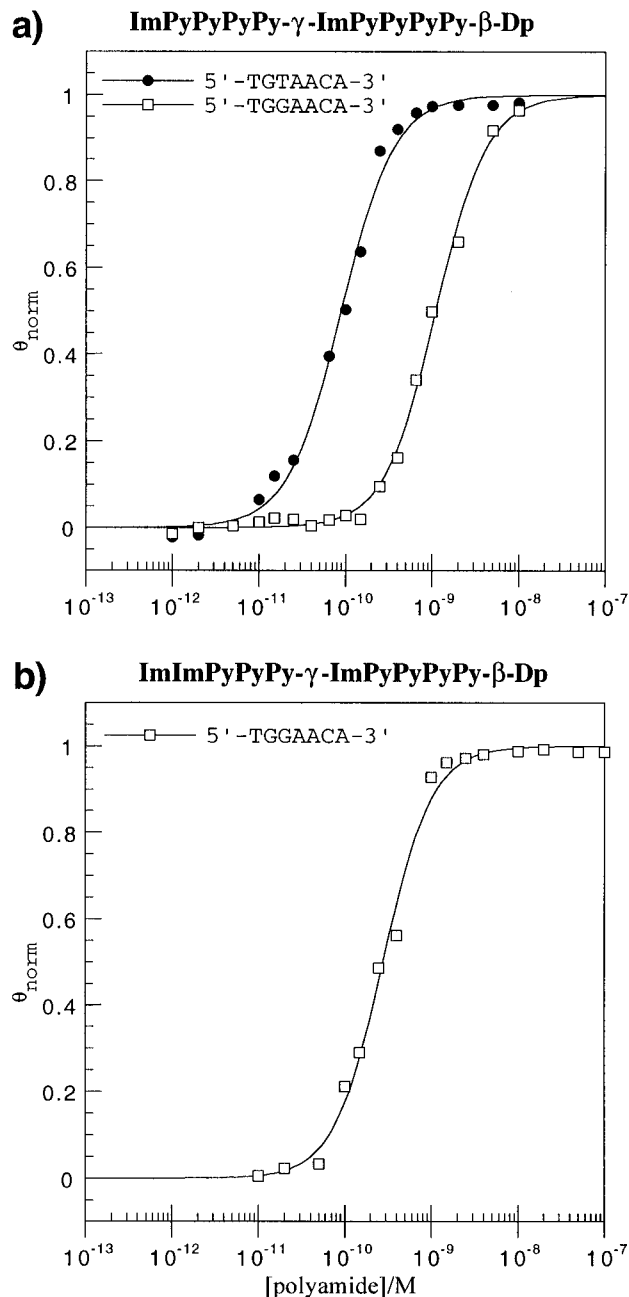


**Figure 11.** Data from the quantitative DNase I footprint titration experiments for the two polyamides, ImPyPyPyPy- $\gamma$ -ImPyPyPyPy- $\beta$ -Dp (top) and ImImPyPyPy- $\gamma$ -ImPyPyPyPy- $\beta$ -Dp (bottom) in complex with the designated sites. The  $\theta_{\text{norm}}$  points were obtained using photostimulable storage phosphor autoradiography and processed as described in the Experimental Section. The data points for 5'-TGTAACA-3' and 5'-TGGAACA-3' sites are indicated by filled circles (●) and open squares (□) respectively. The solid curves are the best-fit Langmuir binding titration isotherms obtained from a nonlinear least squares algorithm using eq 2.

ImImPyPyPy- $\gamma$ -ImPyPyPyPy- $\beta$ -Dp·5'-TGGAACA-3' complex by a factor of 5-fold, a loss in binding energy of  $\sim 1$  kcal/mol.

#### Implications for the Minor Groove Binding Hairpin Motif.

The results presented here reveal that ten-ring polyamides based on  $\gamma$ -linked five-ring subunits expand the binding site size of the hairpin motif, providing a model for the recognition of 7-bp sequences. Recognition of seven base pairs by a ten-ring hairpin represents an upper limit of contiguous rings which will match the curvature of the DNA helix without severe energetic penalty.<sup>15</sup> This observation is consistent with failure of six-ring subunits containing solely pyrrole and imidazole amino

**Table 1.** Equilibrium Association Constants ( $M^{-1}$ ) for Ten-Ring Polyamides<sup>a,b</sup>

binding site	polyamide	
	ImPyPyPyPy- $\gamma$ -ImPyPyPyPy- $\beta$ -Dp	ImImPyPyPy- $\gamma$ -ImPyPyPyPy- $\beta$ -Dp
5'-TGTAACA-3'	$1.2 (\pm 0.2) \times 10^{10}$	$< 1 \times 10^7$
5'-TGGACA-3'	$6.8 (\pm 1.6) \times 10^8$	$3.6 (\pm 2.2) \times 10^9$

<sup>a</sup> Values reported are the mean values obtained from three DNase I footprint titration experiments. The standard deviation for each value is indicated in parentheses. <sup>b</sup> The assays were carried out at 22 °C at pH 7.0 in the presence of 10 mM Tris-HCl, 10 mM KCl, 10 mM MgCl<sub>2</sub>, and 5 mM CaCl<sub>2</sub>.

acids to maintain register as a dimer across the entire length of the minor groove of the helix.<sup>5</sup> Modified hairpin motifs which incorporate flexible linkers to reset the polyamide curvature with the DNA helix will be reported in due course.

## Experimental Section

Dicyclohexylcarbodiimide (DCC), hydroxybenzotriazole (HOBT), 2-(1H-benzotriazole-1-yl)-1,1,3,3-tetramethyluronium hexafluorophosphate (HBTU), and 0.2 mmol/g Boc- $\beta$ -Pam-Resin were purchased from Peptides International. *N,N*-Diisopropylethylamine (DIEA), *N,N*-dimethylformamide (DMF), *N*-methylpyrrolidone (NMP), DMSO/NMP, and acetic anhydride (Ac<sub>2</sub>O) were purchased from Applied Biosystems. Boc- $\gamma$ -aminobutyric acid was from NOVA Biochem, and dichloromethane was reagent grade from EM, thiophenol (PhSH) and ((dimethylamino)propyl)amine were from Aldrich, and trifluoroacetic acid (TFA) was from Halocarbon.

<sup>1</sup>H NMR spectra were recorded on a General Electric-QE NMR spectrometer at 300 MHz in DMSO-*d*<sub>6</sub>, with chemical shifts reported in parts per million relative to residual solvent. UV spectra were measured in water on a Hewlett-Packard Model 8452A diode array spectrophotometer. Matrix-assisted, laser desorption/ionization time of flight mass spectrometry (MALDI-TOF) was performed at the Protein and Peptide Microanalytical Facility at the California Institute of Technology. HPLC analysis was performed on either on a HP 1090M analytical HPLC or a Beckman Gold system using a RAINEN C<sub>18</sub>, Microsorb MV, 5  $\mu$ m, 300  $\times$  4.6 mm reversed phase column in 0.1% (wt/v) TFA with acetonitrile as eluent and a flow rate of 1.0 mL/min, gradient elution 1.25% acetonitrile/min. Preparatory reversed phase HPLC was performed on a Beckman HPLC with a Waters DeltaPak 25  $\times$  100 mm, 100  $\mu$ m C18 column equipped with a guard, 0.1% (wt/v) TFA, 8.0 mL/min, 0.25% acetonitrile/min. 18M $\Omega$  water was obtained from a Millipore MilliQ water purification system, and all buffers were 0.2  $\mu$ m filtered.

**ImPyPyPyPy- $\gamma$ -ImPyPyPyPy- $\beta$ -Dp (1).** ImPyPyPyPy- $\gamma$ -ImPyPyPyPy- $\beta$ -resin was prepared by machine-assisted solid phase synthesis on a 430A Applied Biosystems peptide synthesizer. A sample of resin (240 mg, 0.16 mmol/g<sup>16</sup>) was placed in a 20 mL glass scintillation vial and treated with ((dimethylamino)propyl)amine (2 mL) at 55 °C for 18 h. Resin was removed by filtration, and the filtrate diluted to a total volume of 8 mL with 0.1% (wt/v) aqueous TFA. The resulting crude polyamide/amine solution was purified directly by reversed phase HPLC to provide the trifluoroacetate salt of ImPyPyPyPy- $\gamma$ -ImPyPyPyPy- $\beta$ -Dp (13 mg, 22% recovery) as a white powder. UV (H<sub>2</sub>O)  $\lambda_{\max}$  250, 316 ( $\epsilon$ ) 83300 (calculated based on  $\epsilon = 8333/\text{ring}^{8f}$ ); <sup>1</sup>H NMR (DMSO-*d*<sub>6</sub>)  $\delta$  10.52 (s, 1 H), 10.29 (s, 1 H), 10.04 (s, 1 H), 10.00 (s, 1 H), 9.97 (m, 3 H), 9.92 (m, 2 H), 9.2 (br s, 1 H), 8.06 (m, 3 H), 7.46 (s, 1 H), 7.41 (s, 1 H), 7.29 (d, 1 H,  $J = 1.5$  Hz), 7.27 (d, 1 H), 7.23 (m, 4 H), 7.17 (m, 4 H), 7.07 (m, 5 H), 6.90 (d, 1 H), 6.88 (d, 1 H), 3.99 (s, 3 H), 3.94 (s, 3 H), 3.85 (m, 18 H), 3.79 (s, 6 H), 3.38 (q, 2 H,  $J = 6.0$  Hz), 3.20 (q, 2 H,  $J = 5.1$  Hz), 3.11 (q, 2 H,  $J = 6.3$  Hz),

(15) In support of this, we find that a 12-ring hairpin polyamide motif decreases with regard to both affinity and specificity compared with eight and ten-ring hairpin polyamides.

(16) Resin substitution has been corrected according to  $L_{\text{new}}(\text{mmol/g}) = L_{\text{old}}/(1 + L_{\text{old}}(W_{\text{new}} - W_{\text{old}}) \times 10^{-3})$ , where  $L$  is the loading (mmol of amine per g of resin) and  $W$  is the molecular weight (g mol<sup>-1</sup>) of the polyamide. (See: Barlos, K.; Chatzi, O.; Gatos, D.; Stravropoulos, G. *Int. J. Peptide Protein Res.* **1991**, *37*, 513).

3.00 (q, 2 H,  $J = 4.7$  Hz), 2.72 (d, 6 H,  $J = 4.8$  Hz), 2.35 (m, 4 H), 1.75 (m, 4 H); MALDI-TOF-MS (monoisotopic), 1466.0 (1466.7 calc. for M + H).

**ImImPyPyPy- $\gamma$ -ImPyPyPyPy- $\beta$ -Dp (2).** ImImPyPyPy- $\gamma$ -ImPyPyPyPy- $\beta$ -Pam-Resin was prepared as described for 1. A sample of resin (240 mg, 0.16 mmol/g<sup>16</sup>) was placed in a 20 mL glass scintillation vial and treated with ((dimethylamino)propyl)amine (2 mL) at 55 °C for 18 h. Resin was removed by filtration, and the filtrate diluted to a total volume of 8 mL with 0.1% (wt/v) aqueous TFA. The resulting crude polyamide/amine solution was purified directly by reversed phase HPLC to provide the trifluoroacetate salt of ImImPyPyPy- $\gamma$ -ImPyPyPyPy- $\beta$ -Dp as a white powder (11 mg, 18% recovery). UV (H<sub>2</sub>O)  $\lambda_{\max}$  246, 318 ( $\epsilon$ ) 83 300 (calculated based on  $\epsilon = 8333/\text{ring}^{8f}$ ); <sup>1</sup>H NMR (DMSO-*d*<sub>6</sub>)  $\delta$  10.38 (s, 1 H), 10.28 (s, 1 H), 10.02 (s, 1 H), 9.99 (s, 1 H), 9.96 (s, 1 H), 9.95 (s, 1 H), 9.92 (s, 1 H), 9.91 (s, 2 H), 9.76 (s, 1 H), 9.2 (br s, 1 H), 8.05 (m, 3 H), 7.57 (s, 1 H), 7.46 (m, 2 H), 7.28 (d, 1 H), 7.26 (d, 1 H), 7.16 (m, 4 H), 7.08 (m, 5 H), 6.89 (d, 2 H), 6.88 (d, 2 H), 4.00 (s, 6 H), 3.94 (s, 3 H), 3.85 (m, 15 H), 3.79 (s, 6 H), 3.54 (m, 2 H), 3.19 (m, 2 H), 3.12 (q, 2 H,  $J = 5.7$  Hz), 2.99 (q, 2 H,  $J = 5.1$  Hz), 2.73 (d, 6 H,  $J = 4.8$  Hz), 2.34 (m, 4 H), 1.75 (m, 4 H); MALDI-TOF-MS (monoisotopic), 1466.9 (1466.6 calc. for M + H).

**ImPyPyPyPy- $\gamma$ -ImPyPyPyPy- $\beta$ -Dp-NH<sub>2</sub> (1-NH<sub>2</sub>).** A sample of ImPyPyPyPy- $\gamma$ -ImPyPyPyPy- $\beta$ -resin resin (240 mg, 0.16 mmol/g<sup>16</sup>) was placed in a 20 mL glass scintillation vial and treated with 3,3-diamino-*N*-methylpropylamine (2 mL) at 55 °C for 18 h. Resin was removed by filtration, and the filtrate diluted to a total volume of 8 mL with 0.1% (wt/v) aqueous TFA. The resulting crude polyamide/amine solution was purified directly by reversed phase HPLC to provide the trifluoroacetate salt of ImPyPyPyPy- $\gamma$ -ImPyPyPyPy- $\beta$ -Dp-NH<sub>2</sub> (31 mg, 50% recovery) as a white powder. UV  $\lambda_{\max}$  241, 316; <sup>1</sup>H NMR (DMSO-*d*<sub>6</sub>)  $\delta$  10.53 (s, 1 H), 10.28 (s, 1 H), 10.03 (s, 1 H), 9.99 (s, 1 H), 9.96 (m, 3 H), 9.92 (m, 2 H), 9.6 (br s, 1 H), 8.09 (t, 1 H,  $J = 6.1$  Hz), 8.07 (m, 2 H), 7.9 (br s, 3 H), 7.45 (s, 1 H), 7.41 (s, 1 H), 7.29 (d, 1 H), 7.26 (d, 1 H), 7.23 (m, 4 H), 7.16 (m, 5 H), 7.08 (m, 2 H), 7.06 (m, 2 H), 6.89 (d, 1 H), 6.87 (d, 1 H), 3.98 (s, 3 H), 3.94 (s, 3 H), 3.84 (m, 18 H), 3.79 (s, 6 H), 3.35 (q, 2 H,  $J = 6.3$  Hz), 3.2–3.0 (m, 8 H), 2.85 (q, 2 H,  $J = 5.6$  Hz), 2.72 (d, 3 H,  $J = 4.2$  Hz), 2.34 (m, 4 H), 1.91 (quintet, 2 H,  $J = 7.3$  Hz), 1.78 (m, 4 H). MALDI-TOF MS (monoisotopic), 1509.8 (1509.7 calc. for M + H).

**ImImPyPyPy- $\gamma$ -ImPyPyPyPy- $\beta$ -Dp-NH<sub>2</sub> (2-NH<sub>2</sub>).** A sample of ImImPyPyPy- $\gamma$ -ImPyPyPyPy- $\beta$ -Pam resin resin (240 mg, 0.16 mmol/g<sup>16</sup>) was placed in a 20 mL glass scintillation vial and treated with 3,3-diamino-*N*-methylpropylamine (2 mL) at 55 °C for 18 h. Resin was removed by filtration, and the filtrate diluted to a total volume of 8 mL with 0.1% (wt/v) aqueous TFA. The resulting crude polyamide/amine solution was purified directly by reversed phase HPLC to provide the trifluoroacetate salt of ImImPyPyPy- $\gamma$ -ImPyPyPyPy- $\beta$ -Dp-NH<sub>2</sub> (29 mg, 47% recovery). <sup>1</sup>H NMR (DMSO-*d*<sub>6</sub>)  $\delta$  10.39 (s, 1 H), 10.28 (s, 1 H), 10.03 (s, 1 H), 10.01 (s, 1 H), 10.00 (s, 1 H), 9.97 (s, 1 H), 9.96 (s, 1 H), 9.92 (s, 1 H), 9.82 (s, 1 H), 9.7 (br s, 1 H), 8.11 (t, 1 H,  $J = 5.5$  Hz), 8.07 (m, 2 H), 7.9 (br s, 3 H), 7.57 (s, 1 H), 7.46 (s, 1 H), 7.45 (s, 1 H), 7.28 (d, 1 H,  $J = 1.6$  Hz), 7.26 (d, 1 H,  $J = 1.1$  Hz), 7.23 (m, 2 H), 7.22 (d, 1 H,  $J = 1.3$  Hz), 7.16 (m, 4 H), 7.09 (m, 2 H), 7.07 (d, 1 H,  $J = 1.5$  Hz), 7.06 (d, 1 H,  $J = 1.6$  Hz), 6.89 (d, 1 H,  $J = 1.4$  Hz), 6.87 (d, 1 H), 4.00 (s, 3 H), 3.99 (s, 3 H), 3.94 (s, 3 H), 3.84 (m, 12 H), 3.83 (s, 3 H), 3.79 (m, 6 H), 3.35 (q, 2 H,  $J = 6.1$  Hz), 3.2–3.0 (m, 8 H), 2.86 (q, 2 H,  $J = 6.1$  Hz), 2.72 (d, 3 H,  $J = 4.4$  Hz), 2.34 (m, 4 H), 1.90 (quintet, 2 H,  $J = 7.0$  Hz), 1.78 (m, 4 H). MALDI-TOF-MS (monoisotopic), 1510.9 (1510.7 calc. for M + H).

**ImPyPyPyPy- $\gamma$ -ImPyPyPyPy- $\beta$ -Dp-EDTA (1-E).** EDTA-dianhydride (50 mg) was dissolved by heating at 55 °C for 5 min in a solution of DMSO/NMP (1 mL) and DIEA (1 mL). The dianhydride solution was added to ImPyPyPyPy- $\gamma$ -ImPyPyPyPy- $\beta$ -Dp-NH<sub>2</sub> (1-NH<sub>2</sub>) (10 mg, 6  $\mu$ mol) dissolved in DMSO (750  $\mu$ L). The mixture was heated at 55 °C for 25 min and treated with 0.1 M NaOH (3 mL) for 10 min. Aqueous 0.1% (wt/v) TFA was added to adjust the total volume to 8 mL, and the solution purified directly by HPLC chromatography to provide 1-E as a white powder (2.8 mg, 25% recovery). MALDI-TOF-MS (monoisotopic), 1784.7 (1783.8 calc. for M + H).

**ImImPyPyPy- $\gamma$ -ImPyPyPyPy- $\beta$ -Dp-EDTA (2-E).** Compound 2-E was prepared as a white powder as described for compound 1-E (6



mg, 42% recovery). MALDI-TOF-MS (monoisotopic), 1785.2 (1784.8 calc. for M + H).

**DNA Reagents and Materials.** Restriction endonucleases were purchased from Boehringer-Mannheim or New England Biolabs and were used with their supplied buffers. Sequenase (version 2.0) was obtained from United States Biochemical. Deoxyadenosine and thymidine 5'-[ $\alpha$ - $^{32}$ P]triphosphates and deoxyadenosine 5'-[ $\gamma$ - $^{32}$ P]triphosphate were obtained from Amersham or DuPont NEN. Purified water was obtained by filtering doubly-distilled water through the MilliQ filtration system from Millipore. Sonicated, deproteinized calf thymus DNA and DNase I was acquired from Pharmacia. All other reagents and materials were used as received. All DNA manipulations were performed according to standard protocols.<sup>17</sup>

**Preparation of 3'- and 5'-End-Labeled Restriction Fragments.** Plasmid pJK7 was linearized with *Eco*RI and then treated with either Sequenase (version 2.0), deoxyadenosine 5'-[ $\alpha$ - $^{32}$ P]triphosphate and thymidine 5'-[ $\alpha$ - $^{32}$ P]triphosphate for 3' labeling, or with calf alkaline phosphatase and then 5' labeled with T4 polynucleotide kinase and deoxyadenosine 5'-[ $\gamma$ - $^{32}$ P]triphosphate. The labeled fragment (3' or 5') was then digested with *Pvu*II and loaded onto a 5% nondenaturing polyacrylamide gel. The desired 252 base pair band was visualized by autoradiography and isolated. Chemical sequencing reactions were performed according to published methods.<sup>18</sup>

**MPE·Fe(II) Footprinting.** All reactions were carried out in a volume of 40  $\mu$ L. A polyamide stock solution or water (for reference lanes) was added to an assay buffer where the final concentrations were as follows: 25 mM Tris-acetate (pH 7.0), 10 mM NaCl, 100  $\mu$ M/base pair calf thymus DNA, and 15 kcpm 3'- or 5'-radiolabeled DNA. The solutions were allowed to equilibrate for 16 h. A fresh 50  $\mu$ M MPE·Fe(II) solution was made from 100  $\mu$ L of a 100  $\mu$ M MPE solution and 100  $\mu$ L of a 100  $\mu$ M ferrous ammonium sulfate ( $\text{Fe}(\text{NH}_4)_2(\text{SO}_4)_2 \cdot 6\text{H}_2\text{O}$ ) solution. After the 16 h equilibration, MPE·Fe(II) solution was added to a final concentration of 5  $\mu$ M, and the reactions were equilibrated for 5 min. Cleavage was initiated by the addition of dithiothreitol to a final concentration of 5 mM and allowed to proceed for 14 min. Reactions were stopped by ethanol precipitation, resuspended in 100 mM tris-borate-EDTA/80% formamide loading buffer, denatured at 85  $^\circ\text{C}$  for 10 min, placed on ice, and immediately loaded onto an 8% denaturing polyacrylamide gel (5% cross-link, 7 M urea) at 2000 V for 1.5 h.

**Affinity Cleaving.** All reactions were carried out in a volume of 400  $\mu$ L. A polyamide stock solution or water (for reference lanes) was added to an assay buffer where the final concentrations were as follows: 20 mM HEPES (pH 7.0), 200 mM NaCl, 50  $\mu$ g/mL glycogen, and 15 kcpm 3'- or 5'-radiolabeled DNA. After the reactions were allowed to equilibrate for 16 h, ferrous ammonium sulfate ( $\text{Fe}(\text{NH}_4)_2(\text{SO}_4)_2 \cdot 6\text{H}_2\text{O}$ ), 1  $\mu$ M final concentration, was added. After 15 min, cleavage was initiated by the addition of dithiothreitol to a final concentration of 5 mM and allowed to proceed for 11 min. Reactions were stopped by ethanol precipitation, resuspended in 100 mM Tris-borate-EDTA/80% formamide loading buffer, denatured at 85  $^\circ\text{C}$  for 10 min, placed on ice, and immediately loaded onto an 8% denaturing polyacrylamide gel (5% cross-link, 7 M urea) at 2000 V for 1.5 h.

**DNase I Footprinting.** All reactions were carried out in a volume of 400  $\mu$ L. We note explicitly that no carrier DNA was used in these reactions. A polyamide stock solution or water (for reference lanes) was added to an assay buffer where the final concentrations were: 10 mM Tris-HCl buffer (pH 7.0), 10 mM KCl, 10 mM  $\text{MgCl}_2$ , 5 mM  $\text{CaCl}_2$ , and 15 kcpm 3'-radiolabeled DNA. The solutions were allowed

to equilibrate for a minimum of 72 h at 22  $^\circ\text{C}$ . Cleavage was initiated by the addition of 10  $\mu$ L of a DNase I stock solution (diluted with 1 mM DTT to give a stock concentration of 0.110 u/mL) and was allowed to proceed for 7 min at 22  $^\circ\text{C}$ . The reactions were stopped by the addition of 50  $\mu$ L of a solution containing 2 M NaCl, 150 mM EDTA, and 0.5 mg/mL glycogen, and then ethanol precipitated. The cleavage products were resuspended in 100 mM Tris-borate-EDTA/80% formamide loading buffer, denatured at 85  $^\circ\text{C}$  for 10 min, placed on ice, and immediately loaded onto an 8% denaturing polyacrylamide gel (5% cross-link, 7 M urea) at 2000 V for 1.5 h. The gels were dried under vacuum at 80  $^\circ\text{C}$  and then quantitated using storage phosphor technology.

Equilibrium association constants were determined as previously described.<sup>8</sup> The data were analyzed by performing volume integrations of the 5'-TGTAACA-3' and 5'-TGGAACA-3' sites and a reference site. The apparent DNA target site saturation,  $\theta_{\text{app}}$ , was calculated for each concentration of polyamide using the following equation

$$\theta_{\text{app}} = 1 - \frac{I_{\text{tot}}/I_{\text{ref}}}{I_{\text{tot}}^\circ/I_{\text{ref}}^\circ} \quad (1)$$

where  $I_{\text{tot}}$  and  $I_{\text{ref}}$  are the integrated volumes of the target and reference sites, respectively, and  $I_{\text{tot}}^\circ$  and  $I_{\text{ref}}^\circ$  correspond to those values for a DNase I control lane to which no polyamide has been added. The ( $[L]_{\text{tot}}$ ,  $\theta_{\text{app}}$ ) data points were fit to a Langmuir binding isotherm (eq 2,  $n = 1$ ) by minimizing the difference between  $\theta_{\text{app}}$  and  $\theta_{\text{fit}}$ , using the modified Hill equation

$$\theta_{\text{fit}} = \theta_{\text{min}} + (\theta_{\text{max}} - \theta_{\text{min}}) \frac{K_a^n [L]_{\text{tot}}^n}{1 + K_a^n [L]_{\text{tot}}^n} \quad (2)$$

where  $[L]_{\text{tot}}$  corresponds to the total polyamide concentration,  $K_a$  corresponds to the equilibrium association constant, and  $\theta_{\text{min}}$  and  $\theta_{\text{max}}$  represent the experimentally determined site saturation values when the site is unoccupied or saturated, respectively. Data were fit using a nonlinear least-squares fitting procedure of KaleidaGraph software (version 2.1, Abelbeck software) with  $K_a$ ,  $\theta_{\text{max}}$ , and  $\theta_{\text{min}}$  as the adjustable parameters. All acceptable fits had a correlation coefficient of  $R > 0.98$ . Three sets of acceptable data were used in determining each association constant. All lanes from each gel were used unless visual inspection revealed a data point to be obviously flawed relative to neighboring points. The data were normalized using the following equation

$$\theta_{\text{norm}} = \frac{\theta_{\text{app}} - \theta_{\text{min}}}{\theta_{\text{max}} - \theta_{\text{min}}} \quad (3)$$

**Quantitation by Storage Phosphor Technology Autoradiography.** Photostimulable storage phosphorimaging plates (Kodak Storage Phosphor Screen S0230 obtained from Molecular Dynamics) were pressed flat against gel samples and exposed in the dark at 22  $^\circ\text{C}$  for 12–16 h. A Molecular Dynamics 400S PhosphorImager was used to obtain all data from the storage screens. The data were analyzed by performing volume integrations of all bands using ImageQuant v. 3.2 software.

**Acknowledgment.** We are grateful to the National Institutes of Health (GM-27681) for research support, J. Edward Richter for an undergraduate fellowship to J.M.T., and the Howard Hughes Medical Institute for a predoctoral fellowship to E.E.B. We would like to thank G. M. Hathaway for MALDI-TOF mass spectrometry.

(17) Sambrook, J.; Fritsch, E. F.; Maniatis, T. *Molecular Cloning*; Cold Spring Harbor Laboratory: Cold Spring Harbor, NY, 1989.

(18) (a) Iverson, B. L.; Dervan, P. B. *Nucl. Acids Res.* **1987**, *15*, 7823. (b) Maxam, A. M.; Gilbert, W. S. *Methods Enzymol.* **1980**, *65*, 499.